

FLOW OF VISCOELASTIC FLUIDS THROUGH FLAT CHANNELS AT HIGHER SHEARING STRESSES

V. I. Popov, A. Ya. Roitman,
and E. M. Khabakhpasheva

UDC 532.517.2:532.135

Analyzed are the conditions under which the flow of a viscoelastic fluid becomes unstable and also certain characteristics of such flow.

Unlike the flow of Newtonian or structurally viscous fluids, that of viscoelastic fluids is characterized by several features. Specifically, the laminar flow may become unstable [1] when the parameters which govern the deformation process exceed certain critical values.

The flow of non-Newtonian fluids is most correctly analyzed by experimental methods with an optical visualization of the stream.

The authors used the stroboscopic technique of observation [2] for studying the unstable flow mode in a stream of a concentrated solution and the laminar flow mode in a stream of a weak solution of polymer, both within the stabilization zone. The test fluids were aqueous solutions of polyacrylamide (PAA).

The test apparatus constituted an open-loop system with interchangeable rectangular channels of acrylic glass and the configuration shown in Table 1.

In tests No. 1 and No. 2 the fluid was driven through the channel by means of compressed air. In tests No. 3 and No. 4 the test apparatus included also a constant-level supply tank. Particles of aluminum dust injected into the fluid stream were photographed on still film with the use of an electronic stroboscope and triple lateral flash lights. The tracks of these particles were then processed so as yield instantaneous velocity profiles within the test segment of the channel. Average discharge velocities of the fluid were determined by the volumetric method and by tracing the instantaneous profiles with a planimeter. The pressure was sampled along the channels with the aid of manometer tubes.

The rheological characteristics of the concentrated solution were obtained by means of a model "Rheotest RV" rotary viscometer, while the values of the first difference between normal pressures ($P_{11} - P_{22}$) were measured with a rotameter of the conic-planar type (Fig. 1). The viscosity characteristics of the weak PAA solution were determined with a modified capillary Ubellode viscometer, with which the fluidity curve could be plotted in a single test. All rheological properties were measured at a temperature of $T = 19^\circ\text{C}$.

TABLE 1

Test number	Height, mm	Width, mm	Length, mm	Concentration of the solution, %	Geometry of the channel entrance
1	2.5	25	250	1	Rectangular
2	3	30	600	1	Smooth
3	0.45	10	60	$4 \cdot 10^{-3}$	Rectangular
4	0.5	10	3	$4 \cdot 10^{-3}$	Rectangular

Translated from *Inzhenerno-Fizicheskii Zhurnal*, Vol. 24, No. 5, pp. 836-841, May, 1973. Original article submitted June 21, 1972.

© 1975 Plenum Publishing Corporation, 227 West 17th Street, New York, N.Y. 10011. No part of this publication may be reproduced, stored in a retrieval system, or transmitted, in any form or by any means, electronic, mechanical, photocopying, microfilming, recording or otherwise, without written permission of the publisher. A copy of this article is available from the publisher for \$15.00.

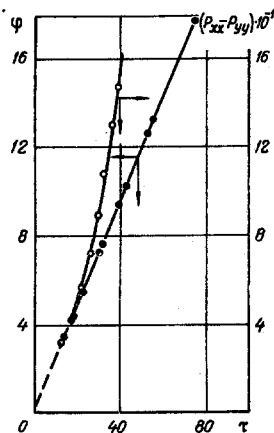


Fig. 1. Rheological characteristics of the 1% aqueous PAA solution: fluidity φ ($\text{m}^2/\text{N} \cdot \text{sec}$), pressure P (N/m^2), τ (N/m^2).

For our tests with the PAA solutions the procedure and the operating channels were first specially checked out on water and water-glycerine mixtures.

In the first and in the second test series (over the 10–75 N/m^2 range of shearing stress in the stabilization zone) we measured the velocity profiles and the pressure drops along a channel, we also photographed the flow pattern at the channel entrance and exit.

In the channel with a rectangular entrance section (test No. 1) with low shearing stresses at the wall ($\tau_S < 20 \text{ N}/\text{m}^2$) the fluid at the entrance flowed in the jet mode (stable) with almost the same characteristics as the flow of water and of water-glycerine mixture. The velocity profiles measured along the channel did not differ from the velocity profiles of structurally viscous fluids [3].

With a subsequent increase in the shearing stress τ_S there appeared inside the pre-entry chamber two vortices and a narrow cone of fluid between them was formed entering the channel. At a short distance from the entrance ($x/d_{\text{eq}} = 0$ to 0.25) the instantaneous velocity profiles revealed their first evidence of asymmetry (Fig. 2a, b).

As the velocity increased further, the flow mode changed substantially. The pre-entry vortices became unstable; portions of the fluid slipped into the channel alternately from the upper and from the lower vortex, while the respective vortex tapered down. As the shearing stress τ_S increased, these oscillations became stronger and the cone of entering fluid "vibrated" while the channel entrance was periodically "blocked." The measurements of velocity profiles in this flow mode (Fig. 2d, $x/d_{\text{eq}} = 33$) revealed momentary up to 25% fluctuations in the flow rate. These fluctuations were measured by tracing with a planimeter the instantaneous velocity profiles which had been plotted for the given channel section. These measurements also revealed a region, a few channel widths away from the entrance (maximum shearing stress $\tau_S = 75 \text{ N}/\text{m}^2$, at $x/d_{\text{eq}} \approx 4$), with very asymmetric instantaneous velocity profiles different at different instants of time. This asymmetry disappeared at distances sufficiently far away from the entrance, but the velocity profiles there assumed a peculiar shape with a distinct flexure point. An extrapolation of the profiles yielded a velocity at the wall other than zero. Special velocity tests at $\tau_S = 75 \text{ N}/\text{m}^2$ yielded a slip velocity possibly as high as 10% of the instantaneous discharge velocity (Fig. 3). The magnitude of the velocity near the wall was determined within a 3% accuracy. A comparison between the measured velocity profile and the one calculated for the usual boundary conditions (without slip) on the basis of a linear $\varphi-\tau$ relation (Fig. 1) is shown in Fig. 4.

The flow pattern at the channel exit also changed, as the shearing stress increased. At low shearing stresses the fluid discharged as a jet. With a higher τ_S , irregularities appeared in the jet like those described earlier in [4]. With a further increase in τ_S , the discharge became pulsating.

The irregularities in the jet of a 1% PAA solution were noted at the channel exit only over a narrow range of shearing stress about the 35 N/m^2 level. For this condition we calculated that the reversible elastic deformation $(P_{11} - P_{22})/\tau_S$ was approximately equal to 4.

Visual observations of the flow near the channel exit and measurements of the velocity profiles at $\tau_S = 50 \text{ N}/\text{m}^2$ revealed a vortex at the lower channel edge, elongated in the direction of flow and reaching up to one fourth the channel height in the vertical direction. This vortex has had its effect on the velocity distribution. The velocity profile measured ahead of the vortex 9 mm before the exit was somewhat asymmetric (Fig. 2c, $x/d_{\text{eq}} = 54$).

The presence of a vortex was perhaps connected with the horizontal position of the channel axis. In a case like this there appears a force in a viscoelastic fluid acting in the direction of the lower exit edge of the channel (an analog of the force appearing in a conic-planar system). A vortex at the exit may be generated by the "supporting" action of this force. In our tests the vortex disappeared when the channel was rotated through 90° (vertical discharge), although the pre-entry flow pattern remained unchanged.

Analogous tests were performed within the same range of shearing stresses in a channel with a smooth entrance section (test No. 2). According to the results of these tests, a change in the entrance

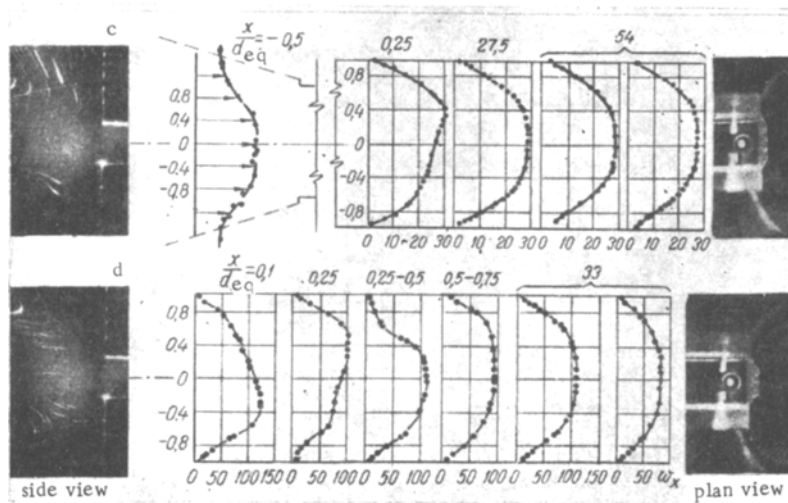
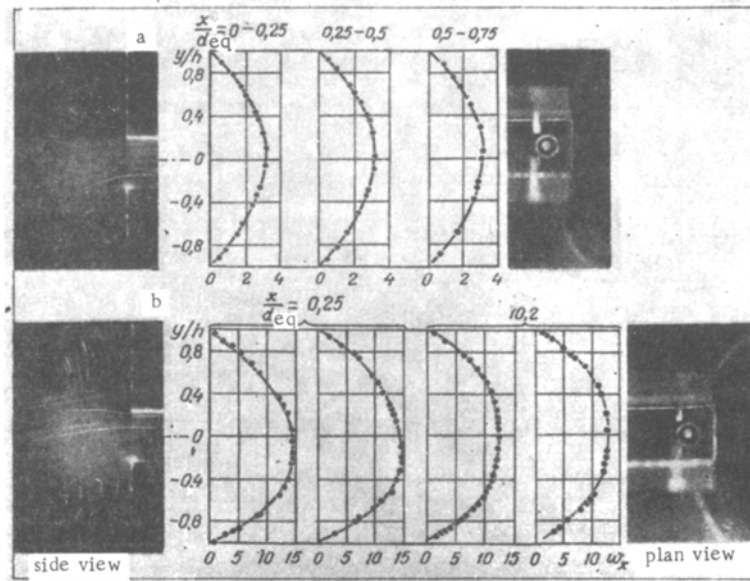


Fig. 2. Velocity distribution (test No. 1) w_x (cm/sec). The velocity profiles at a fixed channel section refer to different instants of time: a) $\tau_S = 20 \text{ N/m}^2$, b) 35 N/m^2 , c) 50 N/m^2 , d) 75 N/m^2 . The photographs show the flow pattern at the channel entrance and exit respectively.

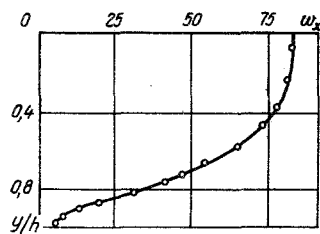


Fig. 3

Fig. 3. Instantaneous velocity profile w_x (cm/sec) at $x/d_{eq} = 23$ and $\tau_S = 75 \text{ N/m}^2$.

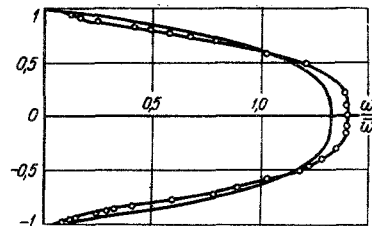


Fig. 4

Fig. 4. Comparison between the calculated velocity profile (curve) and the measured velocity profile (dots), at $x/d_{eq} = 33$ and $\tau_S = 75 \text{ N/m}^2$.

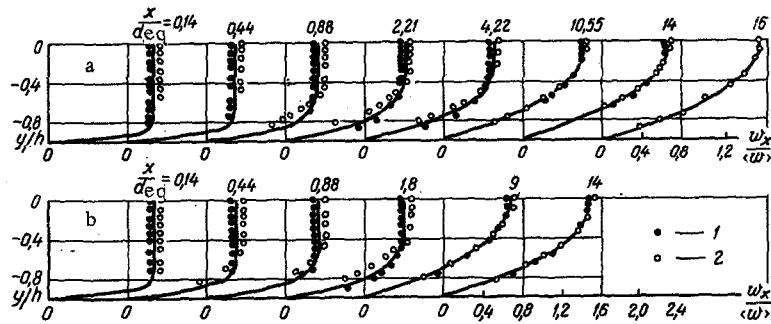


Fig. 5. Velocity profile in a stream of a 0.004% aqueous solution of PAA (test No. 3): 1) test data for the PAA solution, 2) test data for water; curves represent calculations for a Newtonian fluid according to [8]; (a) $Re = 1380$; (b) $Re = 1150$.

geometry from rectangular to smooth tended to stabilize the flow within the entrance zone of the channel.

With the maximum shearing stress ($\tau_S = 70 \text{ N/m}^2$), at locations with a small curvature flat vortices appeared apparently so weak, however, that measurements of the instantaneous velocity profiles in the entrance zone as well as at various distances behind the channel entrance revealed neither a zone of asymmetric velocity profiles nor a zone with pulsations of the instantaneous flow rate.

In tests No. 3 and No. 4 with weak PAA solutions the shearing stress at the channel wall ranged from 25 to 100 N/m^2 and this, judging by the flow curve, made it feasible to perform these tests under an almost constant viscosity ($\mu = 1.2 \text{ N} \cdot \text{sec/m}^2$ at $\tau_S > 15 \text{ N/m}^2$). The velocity profiles measured in the entrance zone of the channel are shown in Fig. 5. These data indicate that the boundary layer in a stream of a PAA solution builds up slower and that the development of a self-adjoint velocity profile requires an initial channel segment which is longer than in the case of a Newtonian fluid. Also additional pressure losses (not incurred in a Newtonian fluid) have been revealed in the initial channel segment. The results of analogous tests with circular channels are shown in [5].

The magnitude of $(P_{11} - P_{22})/\tau_S$, calculated according to the data in [6] with $\tau_S > 25 \text{ N/m}^2$, was greater than 10. Nevertheless, no instability was noted in these tests.

Thus, the flow characteristics of a 1% PAA solution in a channel with a rectangular entrance section changed, as the velocity increased, from stable laminar to pulsating with slip at the wall and distortion of the jet shape at the exit.

One may hypothesize that instability of the viscoelastic flow was due to perturbations seen in the pre-entry zone. Prior to distinct fluctuations of the flow rate, the velocity profile measured in the entering fluid cone (Fig. 2c) had a peculiar shape and became unstable as a result of small perturbations [7]. As the velocity increased, the flow pattern at the entrance became a complex pulsating one. The appreciable effect of entrance perturbations on the instability of a viscoelastic flow was confirmed further by the absence of flow instabilities within the same range of shearing stresses τ_S in the channel with a smooth entrance section.

After the flow of a viscoelastic fluid through horizontal channels under higher shearing stresses has become pulsating, one can distinguish three flow zones: the entrance zone with an asymmetric velocity profile, a stabilized zone, and a vortex zone at the lower edge. In long tubes ($L/d_{eq} \gg 1$) the jet distortion at the exit may be assumed unrelated to the entrance conditions but, rather, a result of perturbations originating from an exit vortex. In short tubes (L/d_{eq} smaller than the relative length of the segment with an asymmetric velocity profile) the jet discharge characteristics at the exit may be related to the conditions of unstable deformation within the entrance zone.

NOTATION

- τ_S is the shearing stress at the channel wall, determined by the pressure drop across the stabilized flow zone, N/m^2 ;
 d_{eq} is the equivalent diameter of the channel;
 x is the distance from the channel entrance, m;

φ is the fluidity, $\text{m}^2/\text{N} \cdot \text{sec}$;
 μ is the dynamic viscosity, $\text{N} \cdot \text{sec}/\text{m}^2$;
 $P_{11} - P_{22}$ is the first difference between normal stresses, N/m^2 .

LITERATURE CITED

1. A. Ya. Malkin and A. L. Leonov, in: Progress in Polymer Rheology [in Russian], Izd. Khimiya (1970).
2. V. V. Orlov, E. S. Mikhailova, and E. M. Khabakhpasheva, Izmeritel. Tekh., No. 3 (1970).
3. Yu. V. Kostylev, V. L. Popov, and E. M. Khabakhpasheva, Prikl. Mekhan. i Tekh. Fiz., No. 1 (1966).
4. V. L. Popov, Inzh. Fiz. Zh., 20, No. 5 (1971).
5. E. S. Mikhailova, A. Ya. Roitman, and E. M. Khabakhpasheva, Izv. Akad. Nauk SSSR, Ser. Tekh. Nauk, No. 13, Ed. 3 (1970).
6. F. A. Seyer and A. B. Metzner, J. AIChE, 15, No. 3 (1969).
7. W. Tollmien, Nachricht. Gesellsch. Wissensch. [German], Göttingen—Berlin (1935).
8. S. M. Targ, Fundamental Problems in the Theory of Laminar Flow [in Russian], Moscow (1952).